NEW APPROACHES TO RECONSTRUCT PAST OCEANIC VARIATIONS IN THE EASTERN EQUATORIAL PACIFIC

By

ANSON HILL-YU CHEUNG

_____

A Thesis Submitted to The Honors College

In Partial Fulfillment of the Bachelors degree
With Honors in

Geosciences

THE UNIVERSITY OF ARIZONA

M A Y 2 0 1 7

Approved by:

_____

Dr. Julia E Cole
Department of Geosciences and Atmospheric Sciences

Abstract

The sea surface temperature (SST) of the Eastern Equatorial Pacific (EEP) can influence the global climate system through different modes of climate variability. Paleoclimate records allow us to study how these regions have changed over long timescales. Yet, there is a lack of paleoclimate record in the EEP, and the fidelity of the proxies commonly used have been questioned. In this study, we use an inductively coupled plasma – optical emission spectrometer (ICP-OES) to generate elemental records (Sr/Ca, Li/Mg, Ba/Ca) from two corals collected in the Galapagos Archipelago and analyze their fidelity to reconstruct past oceanic variations. We show that ICP-OES can measure all targeted elements, but with substantial uncertainty. Sr/Ca remains a robust SST proxy and is more precise and accurate than Li/Mg. Nevertheless, combining Sr/Ca and Li/Mg can help us better reconstruct SST. Although previous work has suggested a link between upwelling and Ba/Ca, we find no such relationship. Our results suggest that reducing analytical uncertainties in ICP-OES can potentially open the door to a rapid approach to carry out multiproxy reconstruction in corals. Our results also caution the use of Ba/Ca as an upwelling indicator.

1. Introduction

The sea surface temperature (SST) of the Eastern Equatorial Pacific (EEP) exerts primary control on global surface temperature (e.g. Halpert and Ropelewski 1992; Wigley 2000) and regional climate (e.g. Ropelewski and Halpert 1987) through different modes of climate variability including the El Niño Southern Oscillation (ENSO) and the Pacific Decadal Oscillation (PDO). With such profound impacts, it is important to understand the evolution of SST in EEP, specifically the dynamics of these climate modes. Rigorous studies over the past decades have shed insights on these two climate modes.

ENSO is known to affect regional and global climates on interannual timescales. During an El Niño event, a weakening of easterly trade wind stimulates propagation of Kelvin waves from the western equatorial Pacific to the EEP, which in turn reduces the slope of the thermocline and suppresses upwelling. The decrease in pressure gradient reinforces the weakening of the trade winds through the Bjerknes feedback and ultimately creates an El Niño condition (e.g. Collins et al. 2010). The reorganization of the ocean and the atmosphere due to El Niño raises the global mean surface temperature (e.g. Halpert and Ropelewski 1992; Wigley 2000) and alters regional climate, for example causing drought in Australia (Cai et al. 2011), pluvial in Southwest United States (Ropelewski and Halpert 1987), and changing tropical cyclone frequencies in the Western North Pacific (Camargo and Sobel 2005; Chan 1985). The opposite spatial pattern and teleconnections happen during a La Niña event.

The PDO can drive global and regional climate on decadal to interdecadal timescales. The mechanism of PDO is less well understood because of the short length of the instrumental data. Nevertheless, Newman et al. (2016) suggest that the PDO involves multiple processes, including atmospheric stochastic forcing, ocean memory, and Rossby wave propagation. In

addition, the low frequency component of ENSO can also drive PDO like variations (e.g. Newman et al. 2003; Newman et al. 2016). Some studies also highlight the importance of the subtropical overturning cells in the Western Pacific on PDO dynamics (Meehl et al. 2013; England et al. 2014). PDO has shown to affect the global hemispheric temperature (e.g. Kosaka and Xie 2013; England et al. 2014) and regional climate such as Southwest United States (e.g. McCabe et al. 2004; Coats et al. 2016).

While analyses based on instrumental data and climate models have allowed us to better characterize ENSO and PDO, future changes of these modes of climate variability remain uncertain, with climate models producing contrasting response of ENSO towards external perturbations (e.g. Collins et al. 2010; Cai et al. 2015) and underestimating low frequency climate variability (e.g. Ault et al. 2012; Laepple and Huybers 2014; England et al. 2014). Disagreements also exist between climate models and instrumental records (e.g. Vecchi and Soden 2007). Part of these disagreements stem from our inability to fully characterize the internal variations of these modes of climate variability and their responses toward external forcings with instrumental records. For instance, Wittenberg (2009) used an unforced global climate model and showed a large variability in ENSO amplitude over a 2000 year period; Cobb et al. (2003; 2013) reconstructed ENSO of the past millennium and the Holocene and showed ENSO exhibited large variability on these two timescales. All these studies highlight the need for long paleoclimate records to further our understanding about these modes of climate variability.

There are numerous coral paleoclimate records in the tropical Pacific (e.g. Shen et al. 1992; Dunbar et al. 1994; Urban et al. 2000; Quinn and Sampson 2002; Cobb et al. 2003; Nurhati et al. 2011; Cobb et al. 2013). However, only few records are located at the EEP (Cole and

Tudhope 2017), and the SST proxies applied in these studies – $^{18}O/^{16}O$ ($\delta^{18}O$) and Sr/Ca – have their own limitations.

$\delta^{18}O$ in corals is a function of ambient SST and $\delta^{18}O$ seawater ($\delta^{18}O_{sw}$). SST and $\delta^{18}O$ are negatively related: corals are more depleted in ^{18}O during warmer conditions and enriched in ^{18}O during cooler conditions (Epstein et al. 1953). $\delta^{18}O$ in corals is also positively related to $\delta^{18}O_{sw}$ – a parameter usually associated with sea surface salinity (SSS) in seawater and the balance between evaporation and precipitation. Since $\delta^{18}O$ is a function of both SST and the hydrological cycle, it can be difficult to isolate the effects of SST for paleoclimate reconstructions. For instance, the freshening in Central and Western Pacific during the late 20th century caused substantial decrease in $\delta^{18}O$ in several coral records, while SST only played a minor role in it (e.g. Cobb et al. 2001; Urban et al. 2000; Nurhati et al. 2009). Some studies attempted to isolate the impacts of SST and SSS by regressing $\delta^{18}O$ onto Sr/Ca and taking the residual as the $\delta^{18}O_{sw}$ component (e.g. Abram et al. 2007). However, this introduces additional error related to the Sr/Ca-SST relationship. $\delta^{18}O$ in the ocean also exhibits large spatial variability. Stevenson et al. (2015) developed an isotope enabled regional ocean model system and showed that mesoscale oceanic processes could alter the $\delta^{18}O$-SSS relationship across the Line Islands, and thus could introduce additional error into $\delta^{18}O$-based paleoclimate reconstruction.

Sr/Ca offers an alternative for SST reconstruction because Sr/Ca is not affected by other environmental factors (e.g. SSS). Numerous studies have demonstrated the Sr/Ca-SST relationship in corals and used such relationship to reconstruct SST (e.g. Beck et al. 1992; Abram et al. 2007; Nurhati et al. 2011). However, other analyses suggest that Sr/Ca is subject

to vital effects (e.g. Cohen et al. 2002; Sinclair et al. 2006; Alpert et al. 2016), which can undermine our ability to accurately reconstruct SST.

With limitations present in $\delta^{18}O$ and Sr/Ca, developing other lines of evidence can help us better reconstruct SST. One potential candidate is Li/Ca, which is temperature dependent in corals (Marriott et al. 2004; Gabitov et al. 2011). However, precipitation rate can also drive Li/Ca changes (Gabitov et al. 2011; Rollion-Bard and Blamart 2015). To minimize vital effects in Li/Ca, several studies used Li/Mg instead as a SST proxy (e.g. Case et al. 2010; Hathorne et al. 2013a; Montagna et al. 2014; Fowell et al. 2016). Their results showed that Li/Mg in different corals could faithfully record SST in different regions.

Coral-based paleoclimate reconstruction usually focuses on SST reconstruction. However, other tracers can offer insights about ocean circulation changes. For example, Ba/Ca is suggested to reflect upwelling, where an increase in upwelling brings more Ba rich deep seawater to the surface (Lea et al. 1989; Shen et al. 1992; Tudhope et al. 1996; Alibert and Kinsley 2008a; Alibert and Kinsley 2008b). Ba/Ca can also be related to terrestrial inputs in coastal regions, where an increase in runoff leads to higher Ba/Ca in corals (e.g. Sinclair 2005; MuCulloch et al. 2003; LaVigne et al. 2016). Analyzing Ba/Ca in parallel with other SST proxies can offer a dynamic perspective on how the ocean has changed. This is particularly useful in studying the EEP because it can reconcile disagreements on the long term change of the tropical Pacific circulation (e.g. Clement et al. 1996; Vecchi et al. 2006; Vecchi and Soden 2007).

In this study, we present two new *Porites spp.* coral records from the Galápagos Archipelago in the Eastern Equatorial Pacific. In contrast to previous studies (e.g. Hathorne et al. 2013a; Montagna et al. 2014; Alibert and Kinsley 2008a), we use an inductively coupled

plasma optical emission spectrometer (ICP-OES) to measure Sr, Ca, Ba, Mg, and Li. We specifically address these questions: 1) whether we can measure all these elements simultaneously with an ICP-OES, which is a more rapid and cheaper method than using inductively coupled plasma mass spectrometer (ICP-MS); 2) whether Li/Mg can be used to faithfully reconstruct SST and thus could be applied in SST reconstruction; 3) whether Ba/Ca in our sites can be used as an upwelling indicator in the EEP.

2. Materials and Methods

2.1. Coral samples and preparation

We present elemental records of 2 modern *Porites spp.* corals (GW10-10; GD15-3-1) that were collected in the Northern part of the Galápagos Archipelago. GW10-10 was live-cored from Shark Bay, Wolf Island (1.39º N, 91.83º W) in May 2010 at 12m depth; GD15-3-1 was live-cored from Wellington Reef, on the eastern side of Darwin Island (1.7º N, 92º W), in January 2015 at 15m depth (Figure 1). A parallel record of Sr/Ca from GW10-10 was presented in Jimenez et al. (in prep.). For both cores, we first halved, slabbed, and cleaned the slabs by sonication in deionized water. Then, we x-rayed each coral slab to establish sampling transects along the coral's primary growth axis (Figure 2). Afterwards, we milled each coral slab at 1 mm increments using a Sherline Computer Numerical control automated benchtop mill with each transect 3 mm wide and 2.5 mm deep. Jimenez et al. (in prep.) analyzed several sections of the GW10-10 slab with a scanning electron microscope at the University of Arizona to determine whether the aragonite has been diagenetically altered. SEM images of GW10-10 display pristine, primary material that has not been affected by diagenesis or alteration (Figure 3).

2.2. ICP-OES analysis

We weighed out 500 – 700 µg of powder and acidified each coral sample powder with 3.5 mL of 5% trace metal grade HNO_3 so that each coral powder had approximately 80 ppm Ca. We measured Sr (422 nm), Mg (280 nm), Ca (315 nm) content in coral powders with a radial torch view and Ba (455 nm), Li (670 nm), Mg (279 nm), and Ca (370 nm) content in coral powders with an axial torch view on a Thermo Electron Corporation iCap 7400 ICP-OES at the University of Arizona. The ability to measure elemental contents in axial torch view enables us to analyze low-concentration elements in corals.

Based on the output of the ICP-OES, we calculated the target elemental ratios (Sr (422 nm)/Ca (315 nm), Ba (455 nm)/Ca (370 nm), Li (670 nm)/Ca (370 nm), Mg (279 nm)/Ca (370 nm)). We then followed the procedure in Schrag (1999) to correct each elemental ratio dataset. We first corrected plasma drift by measuring a reference solution between samples and then readjusting the sample value to remove the drift. Then, we corrected matrix effects by measuring four matrix standards with same M_e/Ca (M_e = metal element) but with stepped Ca concentrations and applying a linear regression that adjusts sample M_e/Ca values based on the M_e/Ca values in the matrix standards. Lastly, we accounted for the offset between the value determined by interlaboratory comparison (Hathorne et al. 2013b) and measured value by normalizing Sr/Ca and Mg/Ca with JCp-1, JCt-1, and an in-house reference MCP (from a western Indian Ocean coral). For Ba/Ca and Li/Ca, we corrected them by applying an offset factor (Ba/Ca: 1.27; Li/Ca: 1.73) calculated from compiled replicate analyses of JCp-1 over all the runs (Cantarero et al. 2017).

2.3. Age model, uncertainty calculation and elemental ratio-SST relationship

To construct age models and calibrate our elemental records, we used the 1° x 1° monthly optimally interpolated sea surface temperature product version 2 (OISST; Reynolds et al. 2002).

We determined the age model for GW10-10 and GD15-3-1 based on seasonal cycles in the Sr/Ca time series. We first identified each year's Sr/Ca minima and tied them to the corresponding SST maxima (March). We then used MATLAB to linearly interpolate the series to monthly time series. Afterwards, we refined the age model by maximizing the correlation between the Sr/Ca monthly series and the SST series.

We calculated the analytic uncertainty for each M_e/Ca in each run by taking 2 standard deviation (2σ) of the measured JCp-1 values. To calculate the analytical uncertainty for Li/Mg, we propagated uncertainty associated with Li/Ca and Mg/Ca by Equation (1):

$$\frac{A}{B} = \frac{A}{B}\sqrt{\left(\frac{\sigma_A}{A}\right)^2 + \left(\frac{\sigma_B}{B}\right)^2} \qquad (1)$$

Where A= Li/Ca, B=Mg/Ca, σ_A=standard deviation in Li/Ca, σ_B = standard deviation in Mg/Ca. We assessed Sr/Ca-SST and Li/Mg-SST relationships by using the weighted least square (WLS) method. We estimated the weight by taking the inverse of the analytical uncertainty variance ($1/\sigma^2$). WLS is a better method than the ordinary least square method because it takes the uncertainty in y-axis (Sr/Ca and Li/Mg) into account when minimizing sum of squared errors.

3. Results

The mean and standard deviation values for JCp-1 are shown in table 1. Mg/Ca is slightly outside the 1σ of the published value while other values are in general agreement with previous studies (Hathorne et al. 2013a; Hathorne et a. 2013b). GW10-10 spans from August 1986 –

February 2010; GD15-3-1 spans from May 1987 – November 2014. Visual inspection on GW10-10 and GD15-3-1 elemental records reveal relationships that are consistent with current knowledge about each elemental ratio (Figures 4 – 6). Sr/Ca, Li/Mg, and Li/Ca in both cores covary; Mg/Ca exhibits an inverse relationship with other elemental ratios. There is no clear relationship between Ba/Ca and other elemental ratios. Sr/Ca to SST and Li/Mg to SST calibration equations are shown in table 2. The slope of GW10-10 Sr/Ca-SST calibration lies well within the range of published calibration values whereas the slope of GD15-3-1 Sr/Ca-SST calibration lies in the lower range of the published calibration values (Corrège 2006). The slopes of both Li/Mg-SST calibrations are slightly lower than values obtained from Japan and Tahiti corals (Hathorne et al. 2013a).

Comparison between the Sr/Ca (Sr/Ca-SST) and Li/Mg (Li/Mg-SST) based modeled SST values from each coral with OISST show that all modeled SST values exhibit certain covariation with OISST (Figure 7). Among the 4 elemental records, Wolf Sr/Ca-SST exhibits the highest correlation (r=0.7673) with OISST. Analytical uncertainty in Sr/Ca-SST is small in both records (maximum GW10-10 2σ: 0.39 °C; maximum GD15-3-1 2σ: 0.51 °C). On the other hand, the analytical uncertainty in Li/Mg-SST varies within the record where it ranges from 1.5 °C to 7.8 °C (2σ) in GW10-10 and 2.0°C to 10.5°C (2σ) in GD15-3-1.

Ba/Ca in both cores show random spikes that do not correspond well with other elemental ratios (Figures 4 – 5). The mean values obtained in this study (GW10-10: 2.15 µmol/mol; GD15-3-1: 2.62 µmol/mol) are lower than the mean value obtained in another Galapagos study from Punta Pitt, where upwelling is stronger (mean value: ~4.4 µmol/mol; Lea et al. 1989; Shen et al. 1992).

4. Discussion

4.1. SST proxies

4.1.1. Fidelity of Sr/Ca and Li/Mg as SST proxies

Despite controversies in applying Sr/Ca as a SST proxy (e.g. Cohen et al. 2002; Alpert et al. 2016), our results indicate a clear relationship between Sr/Ca and SST within this period (Figure 7). Recent studies suggested that Li/Mg may also be applied as a SST proxy (Hathorne et al. 2013a; Montagna et al. 2014). Our results show that Li/Mg covaries with SST (Figures 7); However, the relationship between Li/Mg and SST is weaker than the relationship between Sr/Ca and SST. To understand the underlying causes of the subtle relationship between Li/Mg and SST, we compare Li/Ca and Mg/Ca from both cores with SST (Figure 8). In GW10-10, Li/Ca corresponds well with SST despite the presence of a low frequency cycle that spans the whole record. Mg/Ca tracks the SST seasonal cycle in the earlier part of the record (~1986 – 1998). The relationship, however, breaks down after the 1997 – 1998 El Niño and the mean Mg/Ca values are offset to more positive after the 97 – 98 El Niño. Li/Ca and Mg/Ca behave differently in GD15-3-1 compared to GW10-10. The Mg/Ca in GD15-3-1 closely tracks the SST seasonal cycle; the Li/Ca exhibits strong high frequency variability and a comparatively weak relationship with SST. The variable relationship between Li/Ca, Mg/Ca, and SST can be partially explained by the influence of environmental and biological factors.

The Li/Ca behavior in GW10-10 aligns with previous studies where they suggested a temperature control of Li/Ca in *Porites* corals (Marriott et al. 2004; Hathorne et al. 2013a; Montagna et al. 2014). The secular trend in GW10-10's Li/Ca and the high frequency variability in GD15-3-1's Li/Ca might be driven by biology, since some studies suggested a relationship between precipitation rate and Li/Ca (Gabitov et al. 2011; Rollion-Bard and

Blamart 2015). Our results support such hypothesis, where the mean Li/Ca value is higher in GW10-10 (6.63 µmol/mol; higher growth rate) than GD15-3-1 (5.93 µmol/mol; lower growth rate). Other studies argue that using Li/Mg instead of Li/Ca as a SST proxy can avoid possible vital effects which would impact both elements comparably (Hathorne et al. 2013a; Montagna et al. 2014). In short, the different behavior in Li/Ca in our records do not contradict previous studies.

While the aim of incorporating Mg into the Li/Mg-SST proxy is to minimize the vital effects, Mg/Ca has been suggested to be related to SST (Mitsuguchi et al. 1997). However, subsequent studies showed that the Mg/Ca-SST relationship could be affected by how Mg was attached to the coral skeleton (Meibom et al. 2004; Allison and Finch 2007; Finch and Allison 2008). For example, Allison and Finch (2007) used Secondary Ion Mass Spectrometry (SIMS) to show that Mg was more abundant in centers of calcification (COC). They further suggested that there was no significant relationship between Mg/Ca and SST even after applying a ~77 day running mean to smooth out the high frequency variability. Our data highlight the disagreements seen in earlier work: Mg/Ca appears correlated with SST in the GD-15-3-1 core, but other factors appear to dominate the Mg/SST record from GW10-10. (Figure 5).

By combining Li/Ca and Mg/Ca, it is expected that the vital effects can be minimized (Hathorne et al. 2013a; Montagna et al. 2014). In our case, SST seems to be unable to explain most of the variance in Li/Mg. We suggest that this might be partly due to analytical uncertainty, as the 2σ uncertainty for Li/Ca in our record is up to ~1.38 µmol/mol. Other unknown biological factors, for instance different incorporation mechanisms, can also reduce the coherence between Li/Mg and SST. Finally, the dependence between Li/Mg and SST weakens at higher temperatures, reducing the signal to noise ratio relative to studies that

include non-tropical corals (Montagna et al. 2014). These factors together can contribute to the weak correspondence between Li/Mg and SST in our cores.

4.1.2. Proxy accuracy, precision, and reconstruction

Paleoclimate reconstruction aims for accuracy and precision. Therefore, it is important for a proxy to attain both accuracy and precision. In our study, the analytical uncertainty for Li/Mg is large (Figures 4 – 5). Hence, this suggests that measuring Li and other elements simultaneously by an ICP-OES with accuracy might not be achievable at this stage. Yet, further analysis on the reproducibility in each run suggests that JCp-1 is highly reproducible in some runs (i.e. 2σ = 0.06 mmol/mol; c.f. Hathorne et al. 2013a: 0.04 mmol/mol). Therefore, if we could achieve stability in reproducing the values of the reference material, it would be possible to measure Li simultaneously with other elements in the future. This could be accomplished potentially by increasing sample size, replication, and multi-standard calibration.

Regardless of the analytical precision, if we assume a perfect precision in Sr/Ca and Li/Mg measurements, we can determine the accuracy of each proxy as an SST recorder and draw inference. To estimate the accuracy of each SST proxy, we regress OISST onto each proxy, and calculate the standard error of prediction (SE) by applying Equation (2) (Wilks 2011):

$$SE(\hat{T}) = \sigma_T \sqrt{1 + \frac{1}{N} + \frac{(\mathrm{x}-\bar{x})^2}{\Sigma_{\mathrm{i}=1}(x_i-\bar{x})^2}} \qquad (2)$$

Where N is the sample size, σ_T is the standard error of predicted temperature, $\bar{x}$ is the mean of the elemental record, and x is the sample value. Our results indicate that Sr/Ca has a higher accuracy compared to Li/Mg in both cores (Table 2). Although Li/Mg is a less accurate predictor of SST, the difference between Li/Mg SE and Sr/Ca is subtle. This suggests that Li/Mg can still provide some useful information about the SST.

Single paleoclimate records can be used to reconstruct local climatic conditions; a compilation of multiple proxy records, on the other hand, can be used to reconstruct averaged past temperature variations in the tropical oceans (Wilson et al. 2006; Ault et al. 2009; Tierney et al. 2015), regional continental temperature (e.g. Pages 2k Consortium 2013) or hemispheric temperature (e.g. Mann et al. 2009). These reconstructions can be used to infer dynamics of the past (Pages 2k Consortium 2013; Mann et al. 2009, Abram et al. 2016). One simple and commonly used method for such type of reconstruction is the weighted composite plus scaling (CPS) method. In the weighted CPS method, each proxy record is first z-scored. Then, the weight of each record is determined by the correlation between the proxy record and the target index over the calibration period. Finally, the records are weighted, averaged and regressed onto the target index over the calibration period. Based on different statistics, we can evaluate how well the composite record can reconstruct the target index (e.g. averaged tropical Eastern Equatorial Pacific SST).

To evaluate whether Li/Mg is useful in climate field reconstruction, we select Niño 3 index as the target index, and evaluate the reconstruction skill of 14 different combinations of our elemental records from GW10-10 and GD15-3-1 (Table 3). Since the records from GW10-10 and GD15-3-1 cover slightly different periods, we first choose the common period of these two records (May 1987 – February 2010). We then apply the weighted CPS method to reconstruct Niño 3 index by using 14 different combinations of datasets. For simplicity, we choose the second half of the record (October 1998 – February 2010) as the calibration period and the first half of the record (May 1987 – September 1998) as the validation period. We evaluate the reconstruction skill of each composite record by evaluating the coefficient of determination (r^2) and the root mean squared error (RMSE) during the validation period, the

reduction of error (RE), and the cost of efficiency (CE). r^2 reflects the percent of variance explained by the reconstructed index; RMSE is used to determine the accuracy of the reconstructed index; RE and CE are used to evaluate whether there are skills greater than the calibration and validation period climatology respectively. RE and CE are calculated in equations (3) and (4):

$$RE = 1.0 - [\frac{\Sigma(x_i - \hat{x_i})^2}{\Sigma(x_i - \overline{x_c})^2}] \quad (3)$$

$$CE = 1.0 - [\frac{\Sigma(x_i - \hat{x_i})^2}{\Sigma(x_i - \overline{x_v})^2}] \quad (4)$$

The x_i and $\hat{x_i}$ are the actual and estimated data in year *i* of the validation period; $\overline{x_c}$ and $\overline{x_v}$ are mean of the actual data in the calibration period and validation period respectively. RE and CE ranges from -∞ to 1; RE and CE>0 indicate useful reconstruction skills (Cook et al. 1999; Tierney et al. 2015). Our results show highest reconstruction skill when combining all 4 records together, followed by using GW10-10 Li/Mg, Sr/Ca and GD15-3-1 Sr/Ca (Table 2). Using single elemental records, on the other hand, only yield weak reconstruction skills (Table 2). This suggests that analyzing Li/Mg along with Sr/Ca can potentially help us better constrain SST reconstruction on large spatial scales.

4.2. Upwelling proxy

Comparison between our Ba/Ca records with other elemental ratios show no apparent covariation (Figures 4 – 5). Instead, Ba/Ca occurs in random spikes and are modulated by low frequency variations. We compare our two Ba/Ca records with OISST records, Niño 1+2 and Niño 3 indices, and GODAS temperature at 15m depth on seasonal timescales and show that there are no apparent relationships between these climate variables and Ba/Ca records (Figures 9 – 10). Assuming that these temperature data are reasonable proxies for upwelling, the lack

of relationship indicates that Ba/Ca records from these two corals do not reflect large-scale upwelling conditions in this region. Our results contrast with the conclusions of Lea (1989) and Shen et al (1992), where they found strong relationships between Ba/Ca records in Galapagos coral cores and upwelling as reflected in SST.

Multiple environmental factors can drive Ba/Ca variability in corals. While several studies suggested upwelling variability can drive Ba/Ca variations in corals (e.g. Lea et al. 1989; Shen et al. 1992; Alibert and Kinsley 2008a), terrestrial inputs (e.g. MuCulloch et al. 2003; Sinclair 2006) and temperature (e.g. Lea et al. 1989) can also influence Ba/Ca variability. However, a linear regression between Sr/Ca and Ba/Ca shows that the Ba/Ca records presented in this study do not correlate with temperature (Figure 6). It is also unlikely that terrestrial inputs can pose major influence on our coral records because there is no major river nearby. Interestingly, our mean Ba/Ca values for both records are lower than studies done nearby (Lea et al. 1989; Shen et al. 1992). To evaluate whether upwelling waters can reach the two sites in this study, we can estimate the Ba seawater (Ba_{sw}) in these sites by using the distribution coefficient (D_{Ba}) for Ba in corals, which is approximately ~1.3 (Lea et al. 1989; LaVigne et al. 2016), and compare the Ba_{sw} values with other estimated values nearby. D_{Ba} is calculated by equation (5):

$$D_{Ba} = \left(\frac{Ba}{Ca}\right)_{corals} / \left(\frac{Ba}{Ca}\right)_{SW} \qquad (5)$$

Where Ba/Ca_{corals} is the Ba/Ca content in corals, and Ba/Ca_{sw} is the Ba/Ca content in seawater. The maximum and minimum Ba/Ca_{sw} values calculated from GW10-10 are 30.2 nmol kg^{-1} and 10.2 nmol kg^{-1} respectively; the maximum and minimum Ba/Ca_{sw} values calculated from GD15-3-1 are 28.4 nmol kg^{-1} and 13.9 nmol kg^{-1}. Since Ba_{sw} from GW10-10 and GD15-3-1 are lower than the range suggested by Lea et al. (1989): 33 nmol kg^{-1} and 40 nmol kg^{-1}, we

argue that our records are less impacted by upwelling waters, and thus cannot track upwelling variations accurately. Results from Palacios (2004) support this hypothesis as the SST and a-chlorophyll content in Wolf Island and Darwin Island are different from Punta Pitt, the study site of Lea et al. (1989) and Shen et al. (1992), where upwelling is stronger and average temperatures cooler by ~2°C on average (Figure 11). Wolf and Darwin islands seem to be more influenced by the Panama Bight Influence instead of the upwelling waters from Peruvian coast and the Equatorial Undercurrent (Palacios 2004). Apart from large scale upwelling, regional upwelling might also affect the Ba/Ca ratios in corals. Wolf island experiences periodic thermocline shoaling, which might increase coral's Ba/Ca ratio. Unfortunately, we currently cannot evaluate the relationship between local thermocline shoaling and Ba/Ca in GW10-10 because our incomplete Ba/Ca record does not overlap with the short local temperature logger data.

Several different biological factors can affect the Ba/Ca variability in corals. Tudhope et al. (1996) showed an anomalous Ba/Ca peak at the top of their record and they argued that such peak could be due to the presence of barite or incorporation of Ba in the organic layer. Our record suggests the latter because both coral records have very large spikes at the top of the record (not shown). However, this cannot explain the lack of covariance between Ba/Ca and other environmental factors because below the top 25 mm (GW10-10) and 13 mm (GD15-3-1), our Ba/Ca records have a small range whereas these anomalies generally drive large spikes (at least 1 order of magnitude change). Sinclair (2005) suggested that phytoplankton blooms, the senescence of the cyanobacterium *Trichodesmium* and Ba/Ca in corals could be related. Shen et al. (1992) argued that the long residence time for Ba would allow upwelled waters to retain their Ba signature and advect away from source despite influence from

phytoplankton blooms. However, analysis of these relationships requires a more thorough understanding about the dynamics of phytoplankton in this region, which is outside the scope of this study. Sinclair (2005) further hypothesized that coral mass spawning could cause anomalous Ba behavior in some corals because different sex of corals could influence geochemical signals in corals differently. However, we lack information about the gender of our corals.

Apart from the abiotic and biotic sources, the analytical uncertainty can contribute to the lack of relationship between Ba/Ca and upwelling. The analytical uncertainty in GW10-10 and GD15-3-1 are high (Figures 4 – 5). A tighter constraint of Ba/Ca might improve the relationship between Ba/Ca and upwelling. However, even if we only analyze the period with least analytical uncertainty (GD15-3-1 ~2005 – 2011), there is no direct relationship between Ba/Ca and upwelling (Figure 10). In fact, during this period, the Ba/Ca seemed to spike a year after La Niña events in 2007 and 2010 (2008 and 2011). Although age model offsets might be suspected in this case, the age model is well constrained by other tracers and by banding.

5. Conclusion and Future Work

This study aims to investigate 1) the possibility of using ICP-OES to measure lithium, barium, and other elements simultaneously, 2) the fidelity of Li/Mg in corals as a SST proxy, and 3) whether Ba/Ca in our corals can record upwelling variations. Our results indicate a possibility to measure these targeted elements with an ICP-OES. Li/Mg in our records seem to be temperature dependent. However, Sr/Ca remains as the most reliable SST proxy. Our calibration and validation exercise shows that utilizing multiple elements in a reconstruction model improves SST reconstruction over what is possible with a single tracer. could help us better constrain SST reconstructions. In both cores, Ba/Ca records do not appear to track

upwelling in the EEP, highlighting the importance of understanding mesoscale ocean dynamics and better understanding about the biological impacts on Ba/Ca.

The information of Li/Mg added to SST reconstruction suggests Li/Mg should be analyzed in parallel with other commonly analyzed elemental ratio. This could be achieved by measuring these elements with an ICP-OES. However, current analytical uncertainty associated with Li hinders our ability to further constrain Li/Mg. Therefore, further work is needed in developing a method where the analytical uncertainty could converge. Once this method achieves stability, this method could potentially help us better reconstruct SST in the past and infer past climate dynamics.

Acknowledgements: We thank L. Vetter, C. Shaver, and G. Jimenez for preparing and analyzing samples and helpful discussions. This project is supported by the Honors College Legacy Grant (Thesis) and the National Science Foundation. NOAA_OI_SST_V2 data and GODAS data are provided by the NOAA/OAR/ESRL PSD, Boulder, Colorado, USA, from their Web site at http://www.esrl.noaa.gov/psd/. Niño 1+2 and Niño 3 indices are provided by the NOAA CPC, from their Web site at https://www.esrl.noaa.gov/psd/data/climateindices/list/.

References

Abram, N. J., M. K. Gagan, Z. Liu, W. S. Hantoro, M. T. MuCulloch, and B. W. Suwargadi (2007). Seasonal characteristics of the Indian Ocean Dipole during the Holocene epoch, *Nature*, **445**, 299 – 302, doi: 10.1038/nature05477

Abram, N. J., et al. (2016). Early onset of industrial-era warming acAlross the oceans and continents, *Nature*, **536**, 411 – 418, doi: 10.1038/nature19082.

Alibert, C. and L. Kinsley (2008a). A 170-year Sr/Ca and Ba/Ca coral record from the western Pacific warm pool: 1. What can we learn from an unusual coral record?, *Journal of Geophys. Res.*, **113**, C04008, doi: 10.1029/2006JC003979

Alibert, C. and L. Kinsley (2008b). A 170-year Sr/Ca and Ba/Ca coral record from the western Pacific warm pool: 2. A window into variability of the New Ireland Coastal Undercurrent, *Journal of Geophys. Res.*, **113**, C06006, doi: 10.1029/2007JC004263

Allison, N. and A. A. Finch (2007). High temporal resolution Mg/Ca and Ba/Ca records in modern *Porites lobate* corals, *Geochem. Geophys. Geosyst.*, **8**, Q05001, doi:10.1029/2006GC001477.

Alpert, A. E., A. L. Cohen, D. W. Oppo, T. M. DeCarlo, J. M. Grove, and C. W. Young (2016). Comparison of equatorial Pacific sea surface temperature variability and trends with Sr/Ca records form multiple corals, *Paleoceanography*, **31**, 252 – 265, doi: 10.1002/2015PA002897.

Ault, T. R., J. E. Cole, M. N. Evans, H. Barnett, N. J. Abram, A. W. Tudhope, and B. K. Linsley (2009). Intensified decadal variability in tropical climate during the late 19th century, *Geophys. Res. Lett.*, **36**, L08602, doi: 10.1029/2008GL036924.

Ault, T. R., J. E. Cole, and S. St. George (2012). The amplitude of decadal to multidecadal variability in precipitation simulated by state-of-the-art climate models, *Geophys. Res. Lett.*, **39**, L21705, doi: 10.1029/2012GL053424.

Beck, J. W., R. L. Edwards, E. Ito, F. W. Taylor, J. Recy, F. Rougerie, P. Joannot, and C. Henin (1992). Sea-surface temperature from coral skeletal strontium/calcium ratios, *Science*, **257**, 644 – 647, doi: 10.1126/science.257.5070.644.

Cai, W., P. V. Rensch, T. Cowan, and H. H. Hendon (2011). Teleconnection pathways of ENSO and the IOD and the mechanisms of impacts on Australian Rainfall, *J. Clim.*, **24**, 3910 – 3923, doi: 10.1175/2011JCLI4129.1

Cai, W, et al. (2015). ENSO and greenhouse warming, *Nat. Clim. Change*, **5**, 849 – 859, doi: 10.1038/NCLIMATE2743

Camargo, S. J., and A. H. Sobel (2005). Western North Pacific tropical cyclone intensity and ENSO, *J. Clim.*, **18**, 2996 – 3006.

Cantarero, S I., J. T. I. Tanzil, and N. F. Goodkin (2017). Simultaneous analysis of Ba and Sr to Ca ratios in scleractinian corals by inductively coupled plasma optical emmissions spectrometry, *Limnol. Oceanogr: Methods*, **15**, 116 – 123, doi: 10.1002/lom3.10152.

Case, D. H., L. F. Robinson, M. E. Auro, and A. C. Gagnon (2010). Environmental and biological controls on Mg and Li in deep-sea scleractinian corals, *Earth and Plan. Sci. Lett.*, **300**, 215 – 225, doi: 10.1016/j.epsl.2010.09.029.

Chan, J. C. L. (1985). Tropical cyclone activity in the Northwest Pacific in relation to the El Niño/Southern Oscillation phenomenon, *Mon. Wea. Rev.*, **113**, 599 – 606.

Clement, A. C., R. Seager, M. A. Cane, and S. E. Zebiak (1996). An ocean dynamical thermostat, *J. Clim.*, **9**, 2190 – 2196, doi: *http://dx.doi.org/10.1175/1520-0442(1996)009<2190:AODT>2.0.CO;2*

Coats, S., J. E. Smerdon, B. I. Cook, R. Seager, E. R. Cook, and K. J. Anchukaitis (2016). Internal ocean-atmosphere variability drives megadroughts in Western North America, *Geophys. Res. Lett.*, **43**, 9886 – 9894, doi: 10.1002/2016GL070105.

Cobb, K. M., C. D. Charles, and D. E. Hunter (2001). A central tropical Pacific coral demonstrates Pacific, Indian, and Atlantic decadal climate connections, *Geophys. Res. Lett.*, **28**, 2209 – 2212.

Cobb, K. M., C. D. Charles, H. Cheng, and R. L. Edwards (2003). El Niño/Southern Oscillation and tropical Pacific climate during the last millennium, *Nature*, **424**, 271 – 276.

Cobb, K. M., et al. (2013). Highly variable El Niño-Southern Oscillation throughout the Holocene, *Science*, **339**, 67 – 70, doi: 10.1126/science.1228246

Cohen, A. L., K. E. Owens, G. D. Layne, N. Shimizu (2002). The effect of algal symbionts on the accuracy of Sr/Ca paleotemperatures from coral, *Science*, doi: 10.1126/science.1069330.

Cole, J. E., and A. W. Tudhope (2016). Reef-based reconstructions of Eastern Pacific climate variability, in *Coral Reefs of the Eastern Equatorial Pacific*, vol **8**, edited by P. W. Glynn, D. P. Manzello, and I. C. Enochs, pp 535 – 548, Springer Netherlands.

Collins, M., et al. (2010). The impact of global warming on the tropical Pacific Ocean and El Niño, *Nature Geosci.*, **3**, 391 – 397, doi: 10.1038/NGEO868.

Cook, E. R., D. M. Meko, D. W. Stahle, and M. K. Cleaveland (1999). Drought recosntructions for the continental United States, *J. Clim.*, **12**, 1145 – 1162.

Corrège, T. (2006). Sea surface temperature and salinity reconstruction from coral geochemical tracers, *Paleogeogr. Paleoclimatol. Paleoecol.*, **232**, 408 – 428, doi: 10.1016/j.palaeo.2005.10.014.

Dunbar, R. B., G. M. Wellington, M. W. Colgan, and P. W. Glynn (1994). Eastern Pacific sea surface temperature since 1600 A.D.: The $\delta^{18}O$ record of climate variability in Galápagos corals, *Paleoceanography*, **9**, 291 – 315.

England, M. H., et al. (2014). Recent intensification of wind-driven circulation in the Pacific and the ongoing warming hiatus, *Nat. Clim. Change*, **4**, 222 – 227, doi: 10.1038/NCLIMATE2106.

Epstein, S., R. Buchsbaum, H. A. Lowenstam, and H. C. Urey (1953). Revised carbonate-water isotopic temperature scale, *Geol. Soc. Am. Bull.*, **64**, 1315 – 1326, doi: 10.1130/0016-7606(1953)64[1315:RCITS]2.0.CO;2.

Finch, A. A. and N. Allison (2008). Mg structural state in coral aragonite and implications for the paleoenvironmental proxy, *Geophys. Res. Lett.*, **35**, L08704, doi: 10.1029/2008GL033543.

Fowell, S. E., K. Sandford, J. A. Stewart, K. D. Castillo, J. B. Ries, and G. L. Foster (2016). Intrareef variations in Li/Mg and Sr/Ca sea surface temperature proxies in the Caribbean reef-building coral *Siderastrea siderea*, *Paleoceanography*, **31**, 1315 – 1329, doi: 10.1002/2016PA002968.

Gabitov, R. I., A. K. Schmitt, M. Rosner, K. D. McKeegan, G. A. Gaetani, A. L. Cohen, E. B. Watson, and T. M. Harrison (2011) In situ $\delta^{7}Li$, Li/Ca, and Mg/Ca analyses of synthetic aragonites, *Geochem. Geophys. Geosyst.*, **12**, Q03001, doi: 10.1029/2010GC003322.

Halpert, M. S., and C. F. Ropelewski (1992). Surface temperature patterns associated with the Southern Oscillation, *J. Clim.*, **5**, 577 – 593.

Hathorne, E. C., T. Felis, A. Suzuki, H. Kawahata, and G. Cabioch (2013a). Lithium in the aragonite skeletons of massive *Porites* corals: A new tool to reconstruct tropical sea surface temperature, *Paleoceanography*, **28**, 143 – 152, doi: 10.1029/2012PA002311.

Hathorne, E. C., et al. (2013a). Interlaboratory study for coral Sr/Ca and other element/Ca ratio measurements, *Geochem. Geophys. Geosyst.*, **14**, 3730 – 3750, doi: 10.1002/ggge.20230.

Jimenez, G., J. E. Cole, D.M. Thompson, and A.W. Tudhope, In prep. Galápagos corals reveal late twentieth century warming in the eastern equatorial Pacific. For submission to *Geophysical Research Letters*.

Kosaka, Y. and S-P Xie (2013). Recent global-warming hiatus tied to equatorial Pacific surface cooling, *Nature*, **501**, 403 – 407, doi: 10.1038/nature12534.

Laepple, T., and P. Huybers (2014). Global and regional variability in marine surface temperatures, *Geophys. Res. Lett.*, **41**, 2528 – 2534, doi: 10.1002/2014GL059345.

LaVigne, M., A. G. Grottoli, J. E. Palarady, and R. M. Sherrell (2016). Multi-colony calibrations of coral Ba/Ca with a contemporaneous *in situ* seawater barium record, *Geoch. Cosmochim. Acta*, **179**, 203 – 216, doi: 10.1016/j.gca.2015.12.038.

Lea, D. W., G. T. Shen, and E. A. Boyle (1989). Coralline barium records temporal variability in equatorial Pacific upwelling, *Nature*, **340**, 373 – 376.

Mann, M. E., et al. (2009). Global signatures and dynamical origins of the Little Ice Age and Medieval Climate Anomaly, *Science*, **326**, 1256 – 1259.

Marriott, C. S., G. M. Henderson, N. S. Belshaw, and A. W. Tudhope (2004). Temperature dependence of δ^7Li, δ^{44}Ca and Li/Ca during growth of calcium carbonate, *Earth and Plan. Sci. Lett.*, **222**, 615 – 624, doi: 10.1016/j.epsl.2004.02.031.

McCabe G. J., M. A. Palecki, and J. L. Betancourt (2004). Pacific and Atlantic Ocean influences on multidecadal drought frequency in the United States, *Proc. Natl. Acad. Sci.*, **101**, 4136 – 4141, doi: 10.1073/pnas.0306738101.

Meehl, G. A., A. Hu, J. M. Arblaster, J. Fasullo, and K. E. Trenberth (2013). Externally forced and internally generated decadal climate variability associated with the Interdecadal Pacific Oscillation, *J. Clim.*, **26**, 7298 – 7310, doi: 10.1175/JCLI-D-12-00548.1.

Meibom, A., J. Cuif, F. Hillion, B. R. Constantz, A. Juillet-Leclerc, Y. Dauphin, T. Watanabe, and R. B. Dunbar (2004). Distribution of magnesium in coral skeleton, *Geophys. Res. Lett.*, **31**, L23306, doi: 10.1029/2004GL021313.

Mitsuguchi, T., E. Matsumoto, O. Abe, T. Uchida, P. J. Isdale (1997). Mg/Ca thermometry in coal skeletons, *Science*, **274**, 961 – 963, doi: 10.1126/science.274.5289.961.

Montagna, P., et al. (2014). Li/Mg systematics in scleractinian corals: Calibration of the thermometer, *Geoch. Cosmochim. Acta*, **132**, 288 – 310, doi: 10.1016/j.gca.2014.02.005.

MuCulloch, M., S. Fallon, T. Wyndham, E. Hendy, J. Lough, and D. Barnes (2003). Coral record of increased sediment flux to the inner Great Barrier Reef since European settlement. *Nature*, **421**, 727 – 730.

Newman, M., G. P. Compo, and M. A. Alexander (2003). ENSO-forced variability of the Pacific Decadal Oscillation, *J. Clim.*, **16**, 3853 – 3857.

Newman, M., et al. (2016). The Pacific Decadal Oscillation, revisited, *J. Clim.*, **29**, 4399 – 4427, doi: 10.1175/JCLI-D-15-0508.1.

Nurhati, I. S., K. M. Cobb, C. D. Charles, and R. B. Dunbar (2009). Late 20th century warming and freshening in the central tropical Pacific, *Geophys. Res. Lett.*, **36**, L21606, doi: 10.1029/2009GL030270.

Nurhati, I. S., K. M. Cobb, and E. Di Lorenzo (2011). Decadal-scale SST and salinity variations in the central tropical Pacific: signatures of natural and anthropogenic climate change, *J. Clim.*, **24**, 3294 – 3308, doi: 10.1175/2011JCLI3852.1

Pages 2k Consortium (2013). Continental-scale temperature variability during the past two millennia, *Nature Geosci.*, **6**, 339 – 345, doi: 10.1038/ngeo1797.

Quinn, T. M., and D. E. Sampson (2002). A multiproxy approach to reconstructing sea surface conditions using coral skeleton geochemistry, *Paleoceanography*, **17**, 1062, doi: 10.1029/2000PA000528.

Reynolds, R. W., N. A. Rayner, T. M. Smith, D. C. Stokes, and W. Wang (2002). An improved in situ and satellite SST analysis for climate, *J. Clim.*, **15**, 1609 – 1625.

Reuer, M. K., E. A. Boyle, and J. E. Cole (2003). A mid-twentieth century reduction in tropical upwelling inferred from coralline trace element proxies, *Earth and Plan. Sci. Lett.*, **210**, 437 – 452, doi: 10.1016/S0012-821X(03)00162-6.

Rollion-Bard C. and D. Blamart (2015). Possible controls on Li, Na, and Mg incorporation into aragonite coral skeletons, *Chem. Geol.*, **396**, 98 – 111, doi: 10.1016/j.chemgeo.2014.12.011.

Ropelewski, C. F., and M. S. Halpert (1987). North American precipitation and temperature patterns associated with the El Niño/Southern Oscillation (ENSO), *Mon. Wea. Rev.*, **114**, 2352 – 2452.

Schrag, D. P. (1999). Rapid analysis of high-precision Sr/Ca ratios in corals and other marine carbonates, *Paleoceanography*, **14**, 97 – 102.

Shen, G. T., J. E. Cole, D. W. Lea, L. J. Linn, T. A. McConnaughey, and R. G. Fairbanks (1992). Surface ocean variability at Galápagos from 1936 – 1982: calibration of geochemical tracers in corals, *Paleoceanography*, **7**, 563 – 588.

Sinclair, D. J. (2005). Non-river flood barium signals in the skeletons of corals from coastal Queensland, Australia, *Earth and Plan. Sci. Lett.*, **237**, 354 – 369, doi: 10.1016/j.epsl.2005.06.039.

Stevenson, S., B. S. Powell, M. A. Merrifield, K. M. Cobb, J. Nusbaumer, and D. Noone (2015). Characterizing seawater oxygen isotopic variability in a regional ocean modeling framework: Implications for coral proxy records, *Paleoceanography*, **30**, 1573 – 1593, doi: 10.1002/2015PA002824.

Tierney, J. E., N. J. Abram, K. J. Anchukaitis, M. N. Evans, C. Glry, K. H. Kilbourne, C. P. Saenger, H. C. Wu, and J. Zinke (2015). Tropical sea surface temperatures for the past four centuries reconstructed from coral archives, *Paleoceanography*, **30**, 226 – 252, doi: 10.1002/2014PA002717.

Tudhope, A. W., D. W. Lea, G. B. Shimmield, C. P. Chilcott, and S. Head (1996). Monsoon climate and Arabian sea coastal upwelling recorded in massive corals from Southern Oman, *PALAIOS*, **11**, 347 – 361.

Urban, F. E., J. E. Cole, and J. T. Overpeck (2000). Influence of mean climate change on climate variability from a 155-year tropical Pacific coral record, *Nature*, **407**, 989 – 993

Wigley, T. M. L. (2000). ENSO, volcanoes and record-breaking temperatures, *Geophys. Res. Lett.*, **27**, 4101 – 4104.

Wilks, D. S. (2011). Statistical methods in the atmospheric sciences, Academic Press, Oxford, UK.

Wilson, R., A. Tudhope, P. Brohan, K. Briffa, T. Osborn, and S. Tett (2006). Two-hundred-fifty years of reconstructed and modeled tropical temperature, *Journal of Geophys. Res.*, **111**, C10007, doi: 10.1029/2005JC003188.

	Sr/Ca (mmol/mol)	Ba/Ca (μmol/mol)	Li/Ca (μmol/mol)	Mg/Ca (mmol/mol)	Li/Mg (mmol/mol)
mean	8.885	4.228	7.489	6.202	4.120
1σ	0.055	0.0312	0.622	0.623	0.079

Table 1. external precision (JCp-1) value for each elemental ratio (Sr/Ca, Li/Ca, Mg/Ca, Ba/Ca, Li/Mg)

	correlation	slope	intercept	Standard prediction of error (°C±2σ)
GW10-10 Sr/Ca	0.77	-0.055	10.586	3.31±0.01 °C
GW10-10 Li/Mg	0.48	-0.045	2.622	4.49±0.03 °C
GD15-3-1 Sr/Ca	0.72	-0.043	10.238	3.48±0.01 °C
GD15-3-1 Li/Mg	0.44	-0.032	2.111	4.59±0.02 °C

Table 2. each elemental record's correlation, calibrated slope and intercept with SST. This is calculated by regressing elemental data onto SST (see methods). The standard error of prediction value is calculated by equation (2).

	R^2	RMSE	RE	CE
1+2+3+4	0.673	0.931	0.635	0.617
1+2+3	0.588	1.011	0.570	0.548
1+2+4	0.661	0.934	0.627	0.608
1+3+4	0.597	0.984	0.592	0.572
2+3+4	0.675	0.982	0.594	0.573
1+2	0.581	1.013	0.554	0.531
1+3	0.342	1.219	0.374	0.342
1+4	0.586	0.978	0.591	0.570
2+3	0.564	1.091	0.499	0.473
2+4	0.658	0.993	0.578	0.557
3+4	0.574	1.033	0.518	0.494
1	0.290	1.268	0.302	0.266
2	0.574	1.118	0.457	0.429
3	0.145	1.373	0.149	0.106
4	0.577	1.022	0.521	0.497

Table 3. 1 = Wolf Li/Mg, 2 = Wolf Sr/Ca, 3 = Darwin Li/Mg, 4 = Darwin Sr/Ca. Statistic used (r^2, RMSE, RE, and CE) to measure the skill of 14 different combinations of data used to reconstruct Niño 3 index

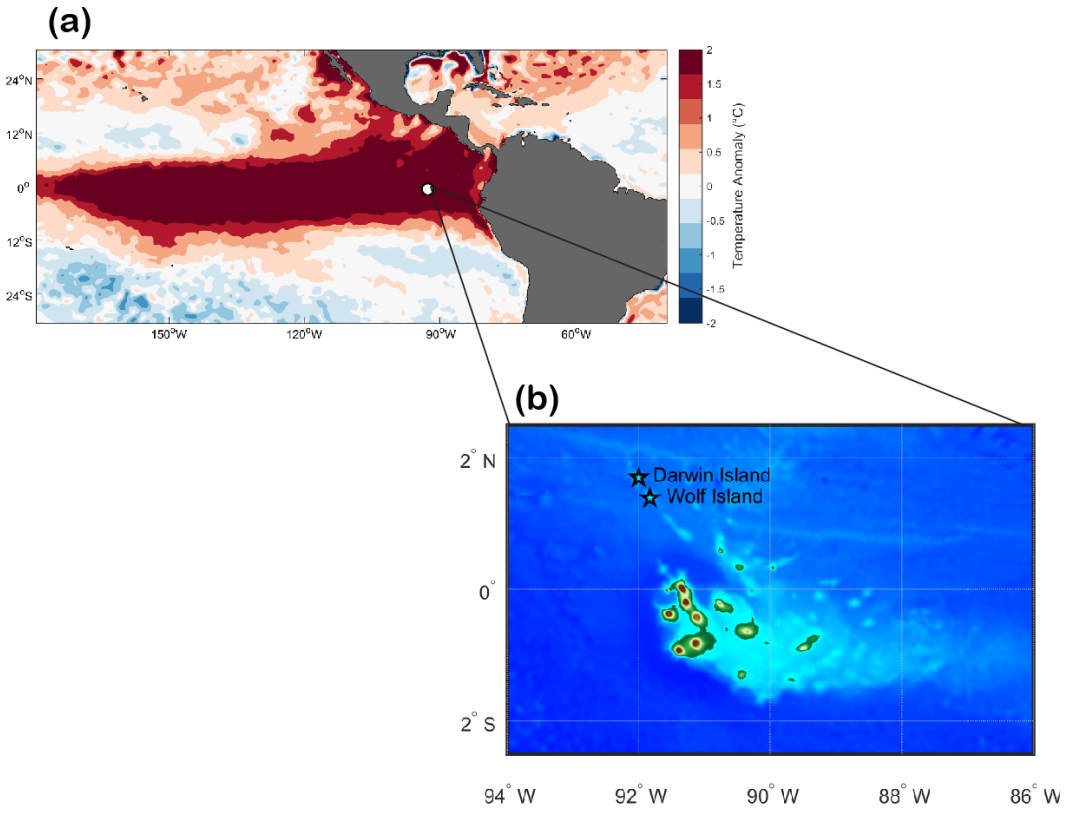

Figure 1a) December – March mean sea surface temperature anomaly during 2015 – 2016 El Niño event from OISST v2 (0.25°x0.25°). b) Bathymetry of the Galápagos Archipelago from National Geophysical Data Center 2-minute Gridded Global Relief Data (ETOPO1), with two stars indicating the two sites where the corals were collected (Darwin Island and Wolf Island).

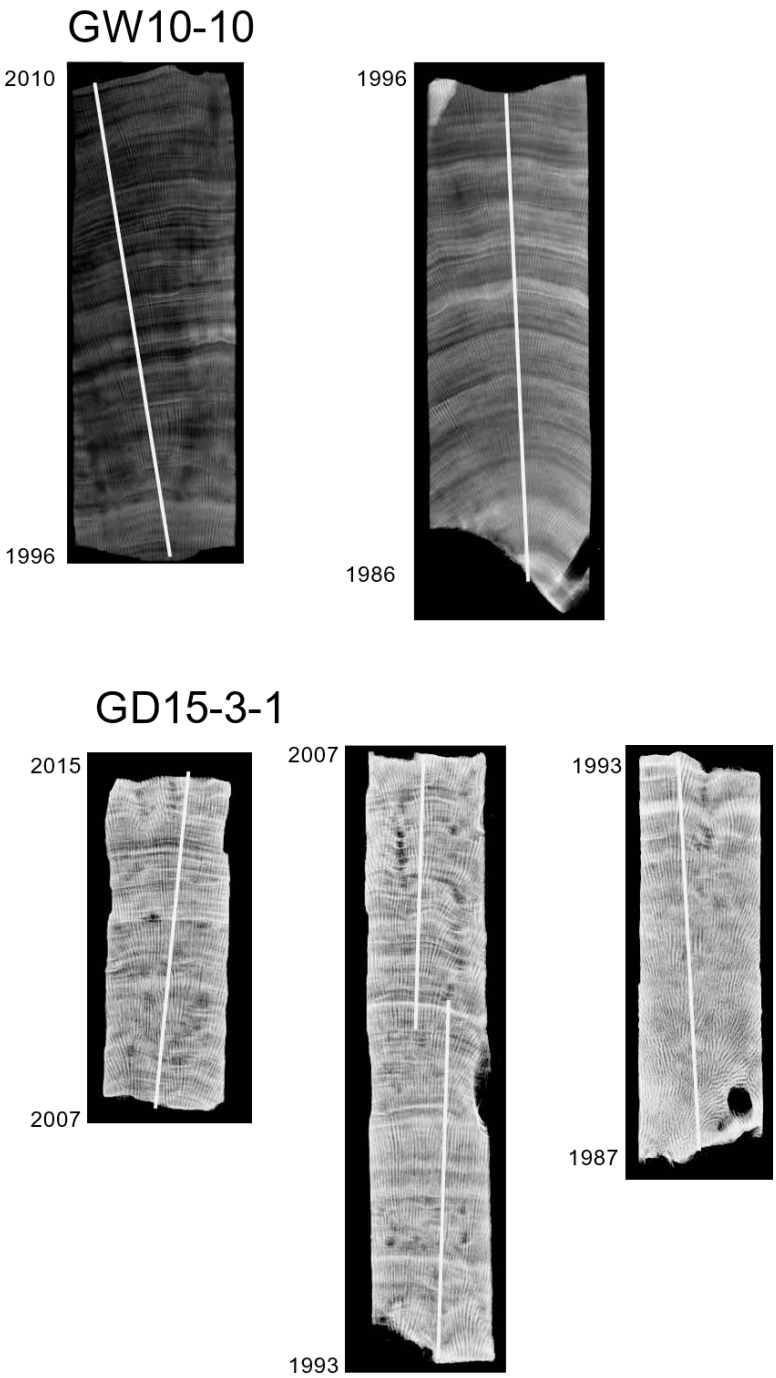

Figure 2. X-ray images of GW10-10 and GD15-3-1. GW10-10 spans from 1986 – 2010 (above) and GD15-3-1 spans from 1987 – 2015 (below). White lines indicate sampling paths, which were taken parallel to the coral's primary growth axis when possible.

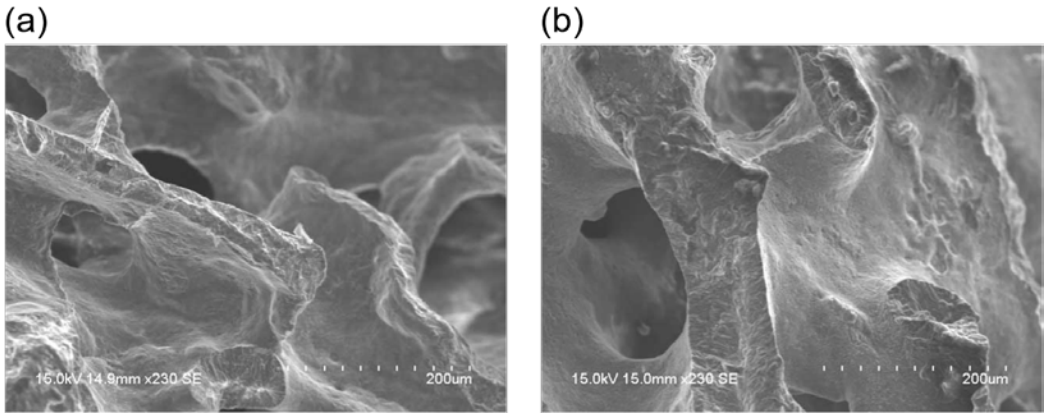

Figure 3. SEM images of Wolf coral core (GW10-10). (a) sample 5 is from the 1997-1998 El Niño cycle, showing primary aragonite. (b) sample 7 is from a sequence in GW10-10 with a strong seasonal cycle, showing primary aragonite (Adapted from Jimenez et al. *in prep.*).

Figure 4. Elemental ratios from GW10-10. The shaded error represents 2σ uncertainty associated with reference material JCp-1.

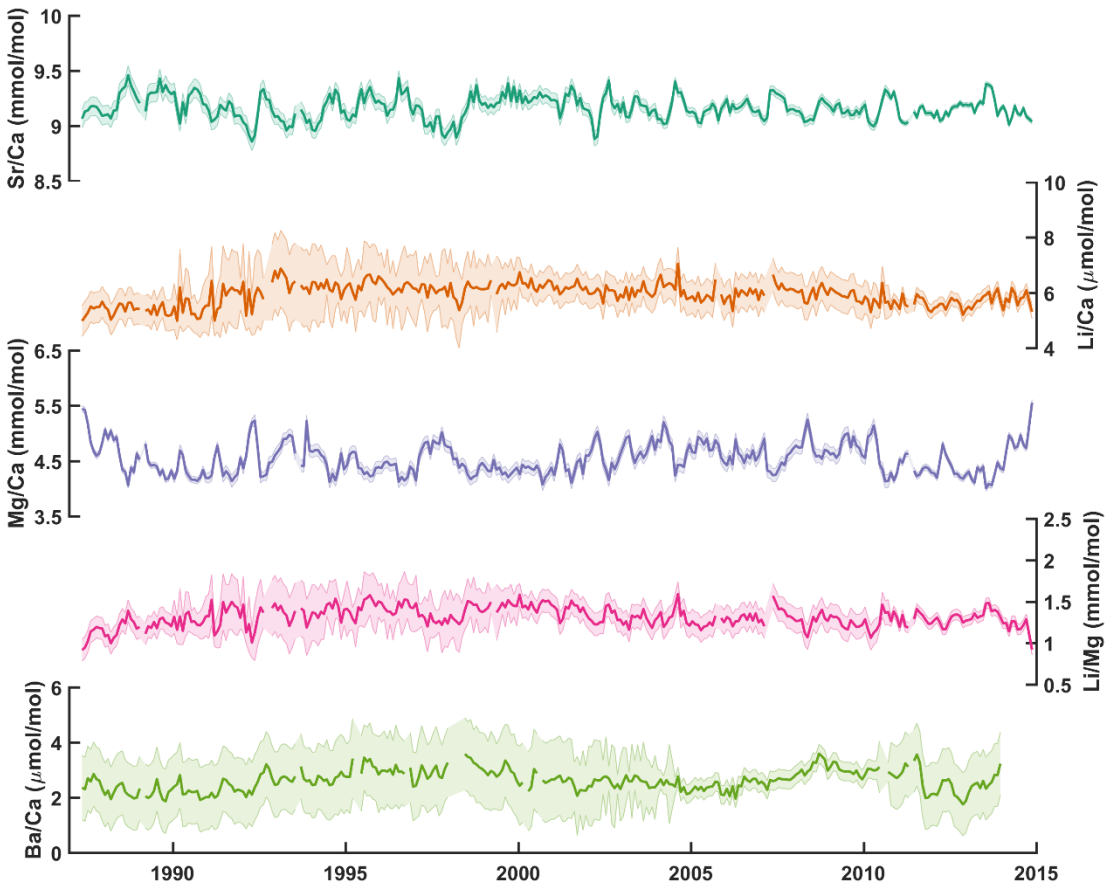

Figure 5. As in figure 4, but from GD15-3-1 instead.

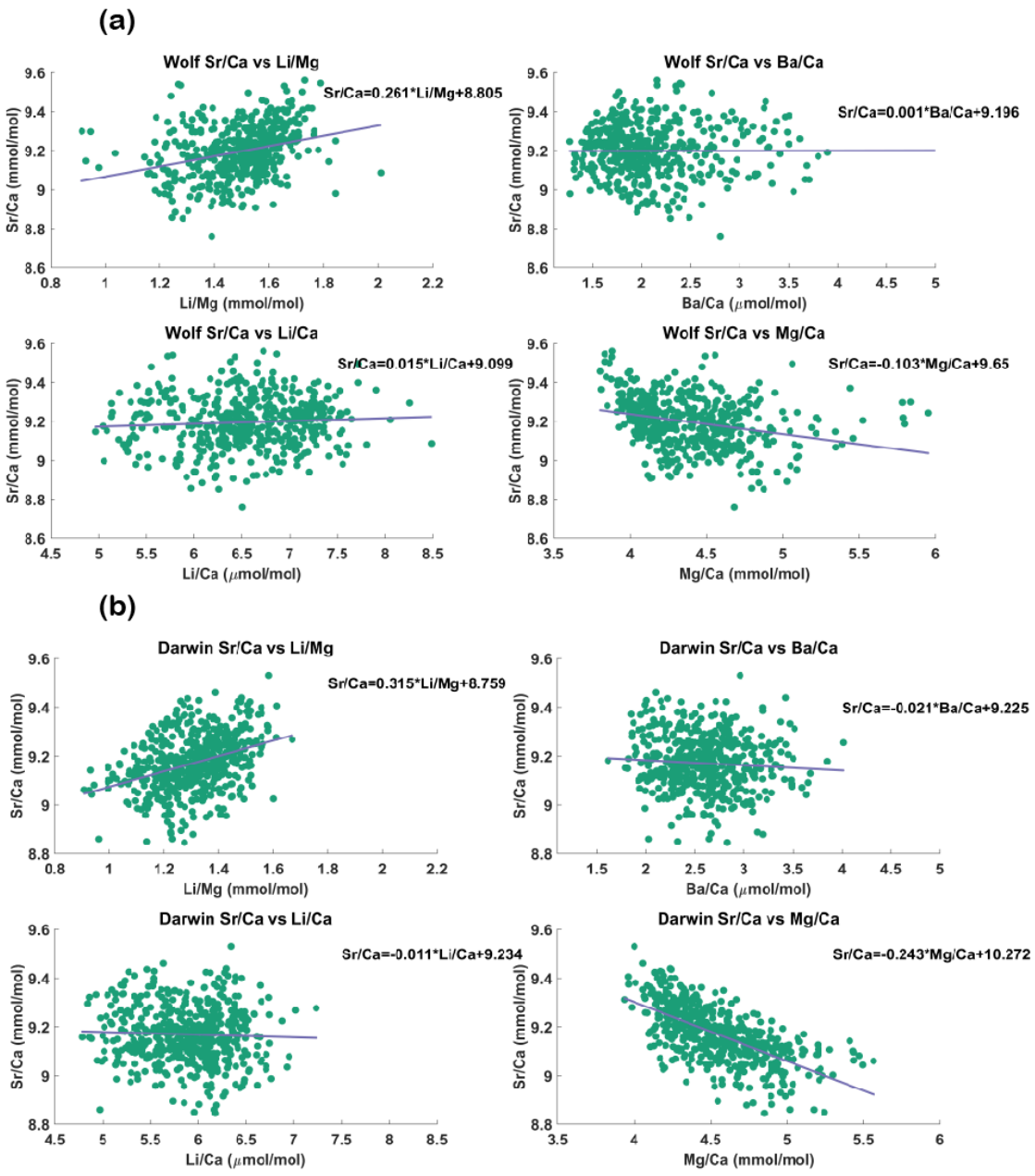

Figure 6. a) Scatter plots of Sr/Ca vs different elemental ratios from GW10-10. b) Scatter plots of Sr/Ca vs different element ratios from GD15-3-1.

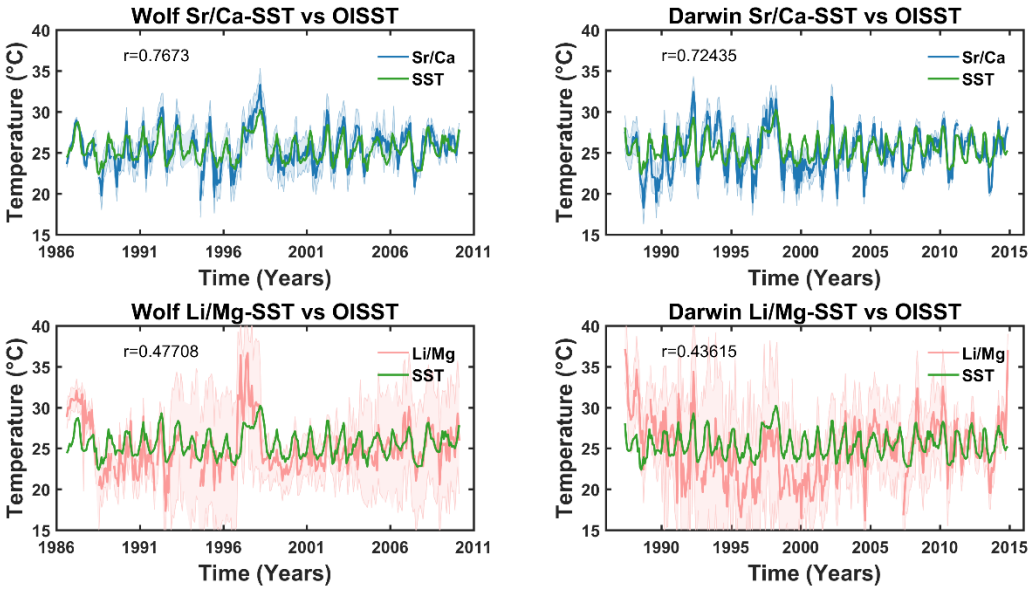

Figure 7. comparison of Sr/Ca and Li/Mg calibrated SST with OISST from Wolf Island and Darwin Island. R indicates the correlation between the calibrated SST and OISST.

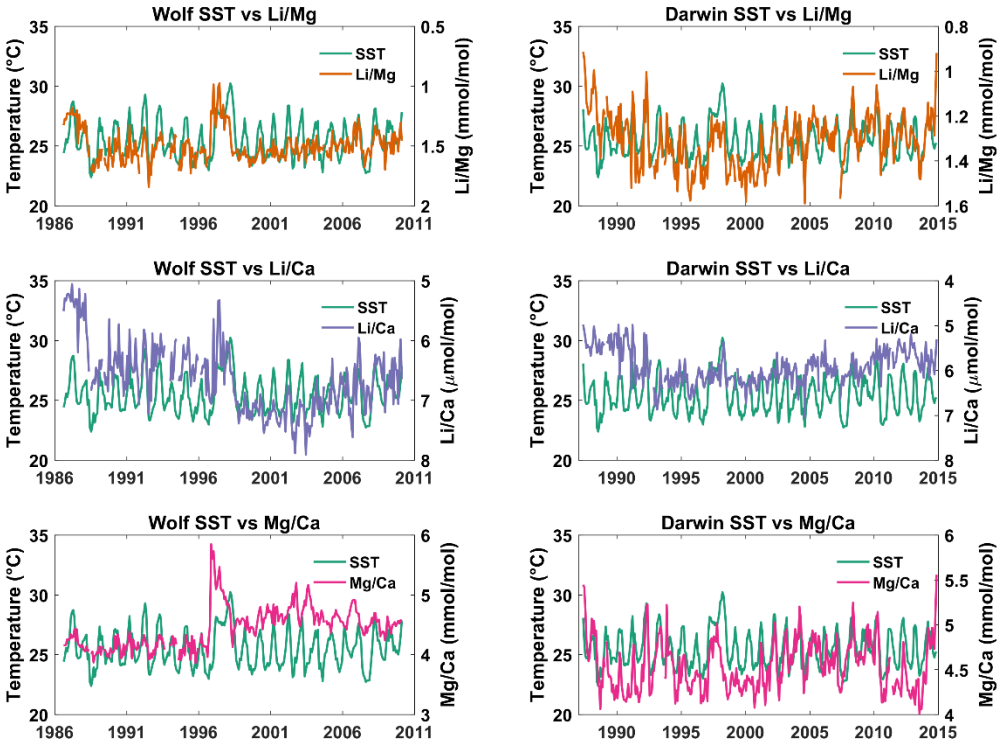

Figure 8. Comparison between OISST and Li/Mg, Li/Ca, and Mg/ Ca from GW10-10 (left panel) and GD15-3-1 (right panel).

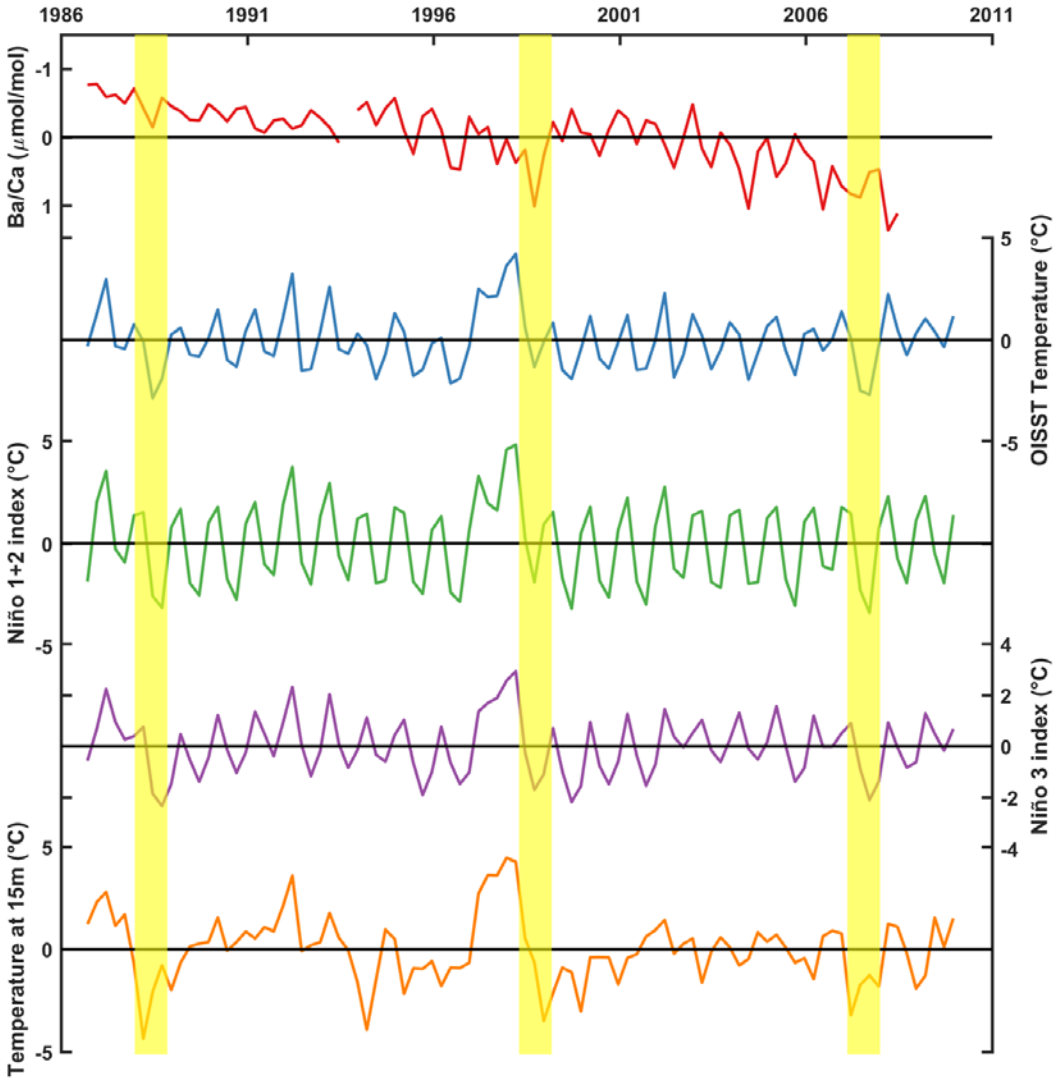

Figure 9. Wolf (GW10-10) seasonal Ba/Ca record, OISST, Niño 1+2, Niño 3 indices, and GODAS reanalysis temperature at 15m depth. The yellow bar highlights the La Niña years (1988, 1999, 2011).

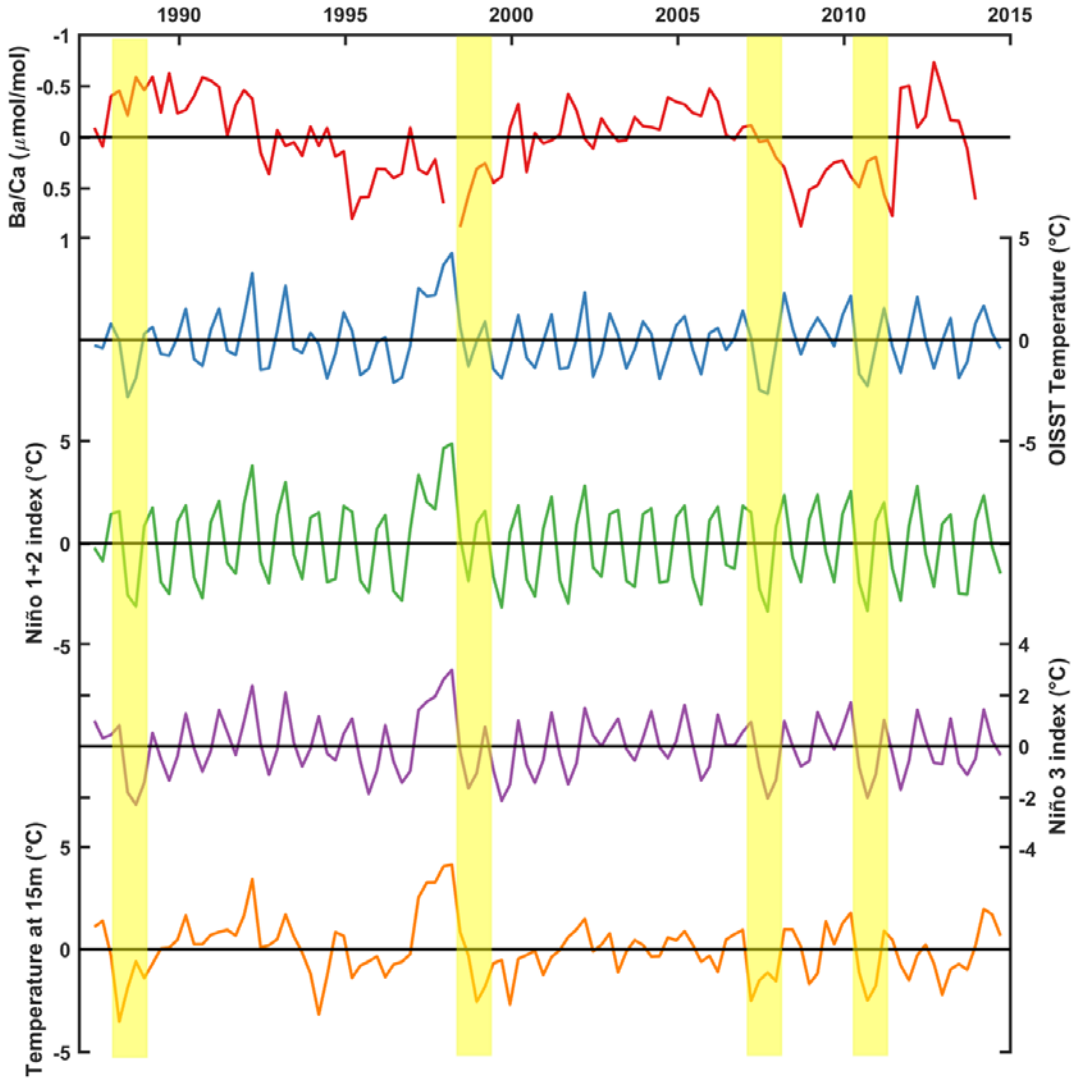

Figure 10. As in figure 9, but with Darwin (GD15-3-1) data displayed instead.

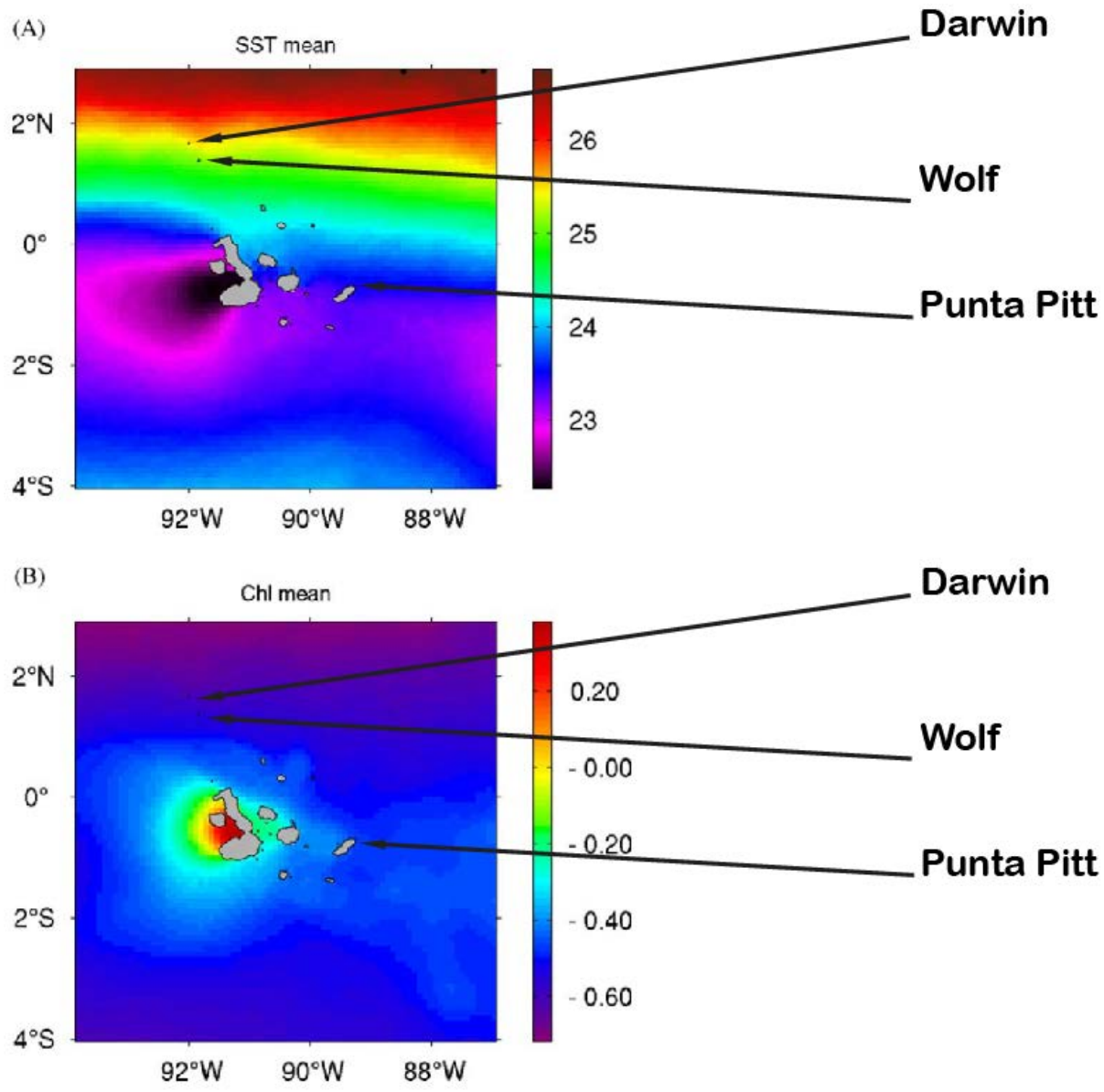

Figure 11. SST mean and a-chlorophyll mean in the Galapagos Island (Adapted from Palacios 2004).